



# Screening of optimum condition for combined modification of ultra-stable Y zeolites using multi-hydroxyl carboxylic acid and phosphate

Xing-wen Chang, Li-feng He, Hai-ning Liang, Xin-mei Liu, Zi-feng Yan\*

State Key Laboratory of Heavy Oil Processing, Key Laboratory of Catalysis CNPC, China University of Petroleum, Qingdao 266555, China

## ARTICLE INFO

Article history:  
Available online 17 March 2010

Keywords:  
Multi-hydroxyl carboxylic acid  
Phosphate  
USY zeolites  
Modification  
Orthogonal experiment

## ABSTRACT

According to the performance requirements of hydrocracking catalyst with high selectivity to middle distillate, multi-hydroxyl carboxylic acid (MHCA) and phosphate (AP) were used to achieve combined dealuminum modification of ultra-stable Y zeolites. The modification effect was influenced by the concentration of MHCA and AP, liquid–liquid ratio, reaction temperature and reaction time. In order to find the optimum modification condition, orthogonal experiment was adopted.  $L_{27}(3^{13})$  orthogonal layout with five factors and three levels was designed and their orthogonal interactions were also included. After investigating the coupling effect of modification systems, the structure and properties of modified samples were characterized by means of BET, FT-IR,  $\text{NH}_3$ -TPD, XRD and TG–DTA. The optimum modification condition was obtained from variance analysis. When the modification was operated under  $100^\circ\text{C}$  lasting 8 h with MHCA 0.4 mol/L, AP 0.2 mol/L and liquid–liquid ratio 1.5, the modified USY samples could have developed secondary pore  $0.184\text{ cm}^3/\text{g}$ , 43.7% of the whole pore volume, and appropriate acid distribution as well as good crystallinity. And then 1 L scale-up test was done. The results showed that the secondary pore volume of modified samples could reach  $0.145\text{ cm}^3/\text{g}$ , 43.9% of the whole pore volume, and the amount and intensity of medium strong acid as well as the thermal stability of modified USY were favorable. Performance evaluation was carried out on a 200 mL fixed-bed single stage hydrogenation unit using Daqing VGO as feedstock. The  $140\text{--}370^\circ\text{C}$  middle distillate yield was 66.04%, and middle distillate selectivity could reach up to 80.43%. Compared with commercial catalyst, the yield and selectivity were increased by 5.62% and 4.05%, respectively. This result showed that combined modification using multi-hydroxyl carboxylic acid and phosphate could meet the need of productive middle distillate in the industrial unit, which predicted it might be a potentially industrialized method of Y zeolites modification.

© 2010 Elsevier B.V. All rights reserved.

## 1. Introduction

In recent years, the demand for high quality middle distillate has been increasing. Especially in China, the demand for aviation kerosene and diesel would increase from actual 38% in 2000 to 45% in 2010—average annual growths of demand for aviation fuel and diesel are 3.1% and 3.3% [1]. Distillate hydrocracking technology can produce middle distillate directly from VGO, taking on many advantages [2], such as extensive raw materials, flexible producing process, good quality of product and high middle distillate yield. The total liquid yield can reach to 96%, even to 98%. In 2008, the hydrocracking capacity of China reached up to 9.805 Mt, while that of the worldwide was 272.664 Mt [3]. Catalyst is the key to hydrocracking technology. Y or USY zeolites are widely applied in

increasing middle distillate yield as hydrocracking additives. Ideal hydrocracking catalysts should have well-developed secondary pore structure, appropriate acid distribution as well as high crystallinity, but the performance of commercial USY is not satisfying. The mesopore volume of commercial Y zeolite is undeveloped and high acid strength and density lead to serious secondary cracking, so modification of Y zeolites is of great significance.

Typical methods to create mesopore of Y zeolites include hydrothermal method [4–8], chemical methods (involving  $\text{SiCl}_4$  high temperature gas-phase method [9,10],  $(\text{NH}_4)_2\text{SiF}_6$  liquid-phase reaction method [11–13],  $\text{NH}_4\text{F}$  [14–17] method and EDTA coordination reaction method [18–21]) and combined methods. Appropriate specification of Si and Al is an essential aspect of obtaining optimal catalyst performance [22]. For hydrothermal method, destruction process of H–Y zeolite into extra-framework aluminum and silicon species is visible and is followed by the structural transformation of H–Y zeolite to kaolinite, silica gel and probable metakaolinite [23]. Extra-framework siliceous admixtures is formed by decomposition of Al-rich and Si-rich regions

\* Corresponding author. Tel.: +86 532 86981296; fax: +86 532 86981295.  
E-mail addresses: [xingwen1100@163.com](mailto:xingwen1100@163.com) (X.-w. Chang),  
[zfyancat@upc.edu.cn](mailto:zfyancat@upc.edu.cn) (Z.-f. Yan).

of the framework and dismutates into an Al rich aluminosilicate and silica gel by steaming treatment [24]. Pore size and acid distribution of individual hydrothermal treatment is unreasonable, so it cannot meet the needs of hydrocracking [25,26]. Modification using  $\text{SiCl}_4$ ,  $(\text{NH}_4)_2\text{SiF}_6$  or  $\text{NH}_4\text{F}$  only undergoes harsh conditions but also causes environmental pollutants [27], such as  $\text{Cl}^-$ ,  $\text{F}^-$ . Dealumination of Y zeolite using  $\text{SiCl}_4$  results in a good distribution of Al and Si atoms in the framework. However, oxygen and chlorine species formed during dealumination process cannot be completely removed. In addition, crystallinity decreases remarkably under high temperature [28].  $(\text{NH}_4)_2\text{SiF}_6$  treatment is highly sensitive to reaction parameters [29] and able to produce a highly crystalline product, but only a minimal contribution of mesopores was observed. For severe dealumination levels, a notable loss of micropores accompanied by the formation of mesopores is noted along with a considerable structural degradation [30]. Recent years, a solid-state dealumination method using crystalline  $(\text{NH}_4)_2\text{SiF}_6$  was employed [31–33]. Although it can improve the efficiency of dealumination, the post treatment is rather complex. For  $\text{NH}_4\text{F}$  method, the addition of fluoride ions to aluminum(III) salts or to zeolites in aqueous solutions produces fluoro complexes of the general form  $[\text{AlF}_n]^{(3-n)-}$  which is of low solubility and are thus hard to remove [34]. Many researchers also tried some inorganic acids, such as hydrochloric acid [35], nitric acid [36] and phosphoric acid [37]. Smieskov et al. [38] found the degree of framework dealumination using HCl depended on the equivalent fraction of protons  $\text{H}^+$  in the solution. To obtain high process selectivity, the extraction had to be carried out at as low  $\text{H}^+$  as possible. There is no structural obvious degradation for  $\text{H}_3\text{PO}_4$ , but its ability to create mesopore is not enough. EDTA coordination reaction is of relative high selectivity to dealumination. Aluminium enrichment in the surface comes from accumulation of non-framework aluminium species which migrate out of the micropore system towards the zeolite surface. The aluminium extraction with EDTA favors the external layers of the crystals [39]. But its operating condition is strict and now only available for laboratory research.

Giving consideration to both mesopore and crystallinity, combined method is adopted. This method is actually the combination of two dealuminum methods or reagents. In 1997,  $\text{H}_2\text{SO}_4$ – $\text{H}_3\text{PO}_4$  combined acid treatment was used by Leiras Gomes et al. [40].  $\text{H}_2\text{SO}_4$  removes non-framework aluminium located in supercavities without attacking the zeolite framework and  $\text{H}_3\text{PO}_4$  could incorporate P in zeolite. This is a good method to create mesopore and meanwhile maintain high crystallinity. But  $\text{H}_2\text{SO}_4$  is a strong acid, it will lead equipment serious corrosion when applied in industry. Triantafyllidis et al. [41] proved combined steaming– $(\text{NH}_4)_2\text{SiF}_6$  could create secondary pore focusing on 3.6 and 15.6 nm. Inspired by EDTA, other organic acid may be advisable, such as oxalic acid [36,42,43] and citric acid [44]. Organic coordination reaction method shows a very attractive potential, because it could be operated in moderate reaction conditions, and no obvious defects are shown in the modified samples. Liu et al. [45] tried the dealumination of Y zeolites with the combination of hydrothermal treatment and oxalic acid. In this work, we attempted to modify commercial USY zeolites by combined modification method using multi-hydroxy carboxylic acid (MHCA) and phosphate (AP) to explore excellent modified routes and laid the technical foundation for hydrocracking catalyst with high selectivity to middle distillate.

lumination of Y zeolites with the combination of hydrothermal treatment and oxalic acid. In this work, we attempted to modify commercial USY zeolites by combined modification method using multi-hydroxy carboxylic acid (MHCA) and phosphate (AP) to explore excellent modified routes and laid the technical foundation for hydrocracking catalyst with high selectivity to middle distillate.

## 2. Experimental

### 2.1. Orthogonal experiment design

#### 2.1.1. Factor selection

Single factor experiments showed that stirring rate had unobvious effect on the experimental results, so a appropriate stirring rate 300 r/min was chosen; Liquid–solid ratio in industrial modification is usually less than 10, and thus we fixed the solid–liquid ratio at 10; when the total volume of two reagents was 120 mL, the amount of their solution was shifted in the relationship and it is convenient to be classified as “liquid–liquid ratio”, a composite factor. Finally, it is just necessary to test the effect of concentrations of MHCA and AP, liquid–liquid ratio, reaction temperature and reaction time on the modification results.

#### 2.1.2. Choosing level

Three levels were selected for each factor based on experience and literature, and the letters in the bracket were in accordance with the corresponding factors (Table 1).

#### 2.1.3. Orthogonal layout design

During the design process of orthogonal layout, if factor A and B were put in the first and second column, respectively, according to the  $L_{27}(3^{13})$  interaction table, the interaction between A and B (represented as  $A \times B$ ) should take up the third and fourth column. Then factor C, D and E were placed in the fifth, sixth and seventh column.  $\text{PO}_4$  hydrolysed by AP might be able to migrate into the zeolite frameworks [37,40], and this process was concerned with time and temperature, so the interactions between B and C (represented as  $B \times C$ ), B and D (represented as  $B \times D$ ), and B and E (represented as  $B \times E$ ) were all taken into consideration. Volume of secondary pore was adopted as the criterion, and thus orthogonal layout was given in the following form (Table 2).

### 2.2. Sample preparation

Firstly, 0.2, 0.3, 0.4 mol/L MHCA solution and 0.2, 0.3, 0.4 mol/L AP solution were prepared, respectively. Each time a fixed quantity of 12 g commercial USY were put into 250 mL three-neck flask. And then according to the orthogonal experiment layout, measured a certain concentration and a certain amount of MHCA and AP solution with 100 mL measuring cylinder. At room temperature, AP solution was first poured into the three-neck flask and

**Table 1**  
Level list of orthogonal experiment of USY modification.

Level	Concentration of MHCA (A), mol/L	Concentration of AP (B), mol/L	Liquid–liquid ratio of MHCA to AP	Reaction time (D), h	Reaction temperature (E), °C
1	0.2	0.2	0.5	4	80
2	0.3	0.3	1	6	90
3	0.4	0.4	1.5	8	100

**Table 2**  
Orthogonal layout of USY modification.

Column	1	2	3	4	5	6	7	8	9	10	11	12	13	14
Factor	A	B	$A \times B$	C	D	E	$B \times C$	$B \times D$	$B \times E$	$B \times C$	$B \times D$	$B \times E$	$B \times E$	Volume of secondary pore, $\text{cm}^3/\text{g}$

mixed with USY while MHCA solution was stored in a dropping funnel which was fixed on a slantwise neck. Installed the stirrer in the central neck, plugged up the other slantwise neck with a glass stopper and set a certain temperature of water bath; when the water bath reached to the set temperature, MHCA solution was added dropwise and finished in 5 min; after thermostatic reaction for a certain time, fetch out the sample, washed and filtrated it to neutral pH; Finally, the sample was put in 110 °C oven, dried for 16 h and grinded after cooling. When the optimum condition was screened out, scale-up test was carried out in 1 L autoclave, setting stirring rate 300 r/min, heating voltage 150 V and external autoclave temperature 155 °C which could maintain internal autoclave temperature 100 °C.

### 2.3. Sample characterization

The nitrogen adsorption of the samples was performed on win 3000 adsorption instrument (Micromeritics Instrument Corporation, U.S.A.) at liquid nitrogen temperature (77.3 K) and the samples were degassed at 573 K under vacuum for 4 h prior to adsorption analysis. Total surface area was calculated using the classical BET method and mesopore surface areas and volumes were evaluated with the method BJH. XRD-ray diffraction analysis was mensurated by X'Pert PRO MPD X-ray diffractometer (Holland PANalytical B.V.), using Cu K $\alpha$  radiation, incident wave length 0.1542 nm, operating voltage 35 kV, operating current 40 mA, scan range of 10°–40° and scan rate of 2°/min. Fourier transform infrared (FT-IR) spectra was given by NEXUS-type FT-IR infrared spectrometer (Nicolet Instrument Corporation, U.S.A.) using self-supporting zeolite plates. Samples were dehydrated at 300 °C under vacuum for 6 h. The interaction with pyridine was then carried out at

room temperature for 24 h, and weakly adsorbed species were removed by evacuation at 90 °C for 1 h. The amount of B acid and L acid were evaluated from the heights of the 1540 and 1450 cm<sup>-1</sup> bands, respectively. NH<sub>3</sub>-TPD characterization was carried out on CHEMBET-3000 TPR/TPD Chemisorption analyzer (Quatachrome Instrument, U.S.A.).

### 2.4. Evaluation of catalyst

Prior to the hydrocracking test, USY sample (10 wt.%) and amorphous silica-alumina (90 wt.%) were mixed together using alumina as peptizator, and then the carrier was produced by extrusion machine in the shape of long column. Ni–W as active component was loaded on carrier by impregnation method. After drying and calcination, the catalyst was prepared.

Performance evaluation of the hydrocracking catalyst was carried out on a 200 mL fixed-bed single stage hydrogenation unit using Daqing VGO as feedstock under the following conditions: pressure 15.0 MPa, volume space velocity 1.5 h<sup>-1</sup>, V(H<sub>2</sub>)/V(oil)=1250 and reaction temperature 385 °C. 100 mL catalyst was loaded. The main properties of Daqing VGO were as follows: Density (20 °C), 0.8519 g/cm<sup>3</sup>, distillate range, 240–500 °C, S content, 827  $\mu$ g/g, N content, 986  $\mu$ g/g.

## 3. Results and discussion

### 3.1. Screening of optimum condition

#### 3.1.1. Results of orthogonal experiment

Hydrocracking catalyst with high selectivity to middle distillate should have well-developed secondary pore structure, and in that

**Table 3**  
Results of orthogonal experiment of USY combined modification.

Column Factor	1 A	2 B	3 A $\times$ B1	4 A $\times$ B2	5 C	6 D	7 E	8 B $\times$ C1	9 B $\times$ D1	10 B $\times$ E1	11 B $\times$ C2	12 B $\times$ D2	13 B $\times$ E2	Volume of secondary pore, cm <sup>3</sup> /g
1	0.2	0.2	1	1	0.5	4	80	1	1	1	1	1	1	0.081
2	0.2	0.2	1	1	1.0	6	90	2	2	2	2	2	2	0.090
3	0.2	0.2	1	1	1.5	8	100	3	3	3	3	3	3	0.142
4	0.2	0.3	2	2	0.5	4	80	2	2	2	3	3	3	0.069
5	0.2	0.3	2	2	1.0	6	90	3	3	3	1	1	1	0.126
6	0.2	0.3	2	2	1.5	8	100	1	1	1	2	2	2	0.127
7	0.2	0.4	3	3	0.5	4	80	3	3	3	2	2	2	0.046
8	0.2	0.4	3	3	1.0	6	90	1	1	1	3	3	3	0.131
9	0.2	0.4	3	3	1.5	8	100	2	2	2	1	1	1	0.108
10	0.3	0.2	2	3	0.5	6	100	1	2	3	1	2	3	0.160
11	0.3	0.2	2	3	1.0	8	80	2	3	1	2	3	1	0.104
12	0.3	0.2	2	3	1.5	4	90	3	1	2	3	1	2	0.104
13	0.3	0.3	3	1	0.5	6	100	2	3	1	3	1	2	0.065
14	0.3	0.3	3	1	1.0	8	80	3	1	2	1	2	3	0.123
15	0.3	0.3	3	1	1.5	4	90	1	2	3	2	3	1	0.118
16	0.3	0.4	1	2	0.5	6	100	3	1	2	2	3	1	0.104
17	0.3	0.4	1	2	1.0	8	80	1	2	3	3	1	2	0.110
18	0.3	0.4	1	2	1.5	4	90	2	3	1	1	2	3	0.096
19	0.4	0.2	3	2	0.5	8	90	1	3	2	1	3	2	0.148
20	0.4	0.2	3	2	1.0	4	100	2	1	3	2	1	3	0.131
21	0.4	0.2	3	2	1.5	6	80	3	2	1	3	2	1	0.128
22	0.4	0.3	1	3	0.5	8	90	2	1	3	3	2	1	0.117
23	0.4	0.3	1	3	1.0	4	100	3	2	1	1	3	2	0.107
24	0.4	0.3	1	3	1.5	6	80	1	3	2	2	1	3	0.109
25	0.4	0.4	2	1	0.5	8	90	3	2	1	2	1	3	0.118
26	0.4	0.4	2	1	1.0	4	100	1	3	2	3	2	1	0.109
27	0.4	0.4	2	1	1.5	6	80	2	1	3	1	3	2	0.111
$K_{j1}$	0.102	0.121	0.106	0.106	0.101	0.096	0.098	0.121	0.114	0.106	0.118	0.106	0.111	T=2.983
$K_{j2}$	0.109	0.107	0.114	0.116	0.115	0.114	0.116	0.099	0.112	0.107	0.105	0.111	0.101	
$K_{j3}$	0.120	0.104	0.111	0.110	0.116	0.122	0.117	0.111	0.105	0.118	0.108	0.115	0.120	
$R_j$	0.018	0.017	0.008	0.010	0.015	0.026	0.019	0.022	0.009	0.012	0.013	0.009	0.019	

According to the experimental design and arrangement, 27 experiments were done for systematic investigation and each result  $y_i$  ( $i = 1, 2, \dots, 27$ ) was filled in the corresponding place of the form.  $T$  was the sum of 27 experimental results,  $T = \sum_{i=1}^{27} y_i$ .  $K_{j1}$ ,  $K_{j2}$ ,  $K_{j3}$  was the average value of the first, second and third level of column  $j$ , respectively ( $j = A, B, A \times B1, \dots, B \times E2$ ).  $R_j$  was the range between maximum and minimum,  $R_j = \{K_{j1}, K_{j2}, K_{j3}\}_{\max} - \{K_{j1}, K_{j2}, K_{j3}\}_{\min}$  ( $j = A, B, A \times B1, \dots, B \times E2$ ).

**Table 4**

Variance analysis of orthogonal experiment.

Factor	Sum of squares of deviations, $S_j^2$	Degree of freedom, $f_j$	Mean square deviation, $MS_j$	F value	Significance
A	$1.37 \times 10^{-3}$	2	$6.85 \times 10^{-4}$	3.70	(*)
B	$1.52 \times 10^{-3}$	2	$7.60 \times 10^{-4}$	4.11	(*)
C	$1.26 \times 10^{-3}$	2	$6.30 \times 10^{-4}$	3.40	(*)
D	$3.21 \times 10^{-3}$	2	$1.60 \times 10^{-3}$	8.65	**
E	$2.15 \times 10^{-3}$	2	$1.08 \times 10^{-3}$	5.84	*
B × C	$3.03 \times 10^{-3}$	4	$7.58 \times 10^{-4}$	4.10	*
B × E	$2.34 \times 10^{-3}$	4	$5.85 \times 10^{-4}$	3.16	(*)
e	$1.48 \times 10^{-3}$	8	$1.85 \times 10^{-4}$	–	

The symbols “\*\*\*”, “\*\*” and “(\*)” indicated the factors or interactions that was highly significant, significant and less significant to experimental results.

case, both the reactants and products could diffuse rapidly from catalyst to avoid secondary cracking and thus improve middle distillate selectivity and yield of liquid oil. So it was reasonable that volume of secondary pore was adopted as criterion. The results were given in Table 3. We aimed to figure out the optimum condition that was most favorable to create mesopore, and variance analysis should be done.

### 3.1.2. Variance analysis

For the variance analysis of three-level orthogonal experiment, sum of squares of deviations ( $S_j^2$ ) of each factor was given as follows:

$$S_j^2 = (T_{j1}^2 + T_{j2}^2 + T_{j3}^2)/9 - T^2/27$$

$T_{j1}, T_{j2}, T_{j3}$  were the sum of the first, second and third level of column  $j$  in Table 3, respectively ( $j=A, B, A \times B1, \dots, B \times E2$ ).

$$S_{A \times B}^2 = S_{A \times B1}^2 + S_{A \times B2}^2, \quad S_{B \times C}^2 = S_{B \times C1}^2 + S_{B \times C2}^2,$$

$$S_{B \times D}^2 = S_{B \times D1}^2 + S_{B \times D2}^2, \quad S_{B \times E}^2 = S_{B \times E1}^2 + S_{B \times E2}^2$$

In principle, variance analysis could not be carried out for the full list orthogonal layout, but there was an alternative method to regard the sum of squares of deviations of a certain column or the average value of that of several columns which was or were obviously smaller than others as the error source. In this experiment,  $A \times B$  and  $B \times D$  were adopted as the variance source, so the sum of squares of deviations of the error was given as follows:

$$S_e^2 = S_{A \times B}^2 + S_{B \times D}^2 = 6.84 \times 10^{-4} + 8.00 \times 10^{-4} = 1.48 \times 10^{-3}$$

Degree of freedom of each factor  $f_j$  was given in Table 4.

Mean square deviation ( $MS_j$ ) was formulated in the form of  $MS_j = S_j^2/f_j$ .

The significance of each factor was judged according to  $F$  value, which was calculated by  $F_j = MS_j/MS_e$  (here  $j=A, B, C, D, E, B \times C, B \times E$ ).

According to  $F$  distribution table:  $F_{0.01}(2, 8)=8.65$ ,  $F_{0.05}(2, 8)=4.46$ ,  $F_{0.10}(2, 8)=3.11$ ;  $F_{0.01}(4, 8)=7.01$ ,  $F_{0.05}(4, 8)=3.84$ ,  $F_{0.10}(4, 8)=2.81$ . It was obviously that factor  $D$  was highly significant while factor  $E$  and interaction  $B \times C$  were significant, and  $A, B, C, B \times E$  were less significant to the results.

### 3.1.3. Interaction analysis

Just as mentioned above, volume of secondary pore was adopted as criterion, and it was evident that when the concentration of AP ( $B$ ) was 0.2 mol/L, liquid–liquid ratio ( $C$ ) was 0.5, volume of secondary pore could reach to maximal 0.130 cm<sup>3</sup>/g (Table 5), so the factor combination  $B1C1$  was chosen.

Still the same case, it was obvious that when the concentration of AP ( $B$ ) was 0.2 mol/L, reaction time ( $E$ ) was 100 °C, volume of secondary pore could reach to maximal 0.144 cm<sup>3</sup>/g (Table 6), so the factor combination  $B1E3$  was chosen.

**Table 5**Interaction list between  $B$  and  $C$ .

C	B		
	0.2	0.3	0.4
0.5	0.130	0.083	0.090
1.0	0.109	0.119	0.117
1.5	0.125	0.118	0.105

**Table 6**Interaction list between  $B$  and  $E$ .

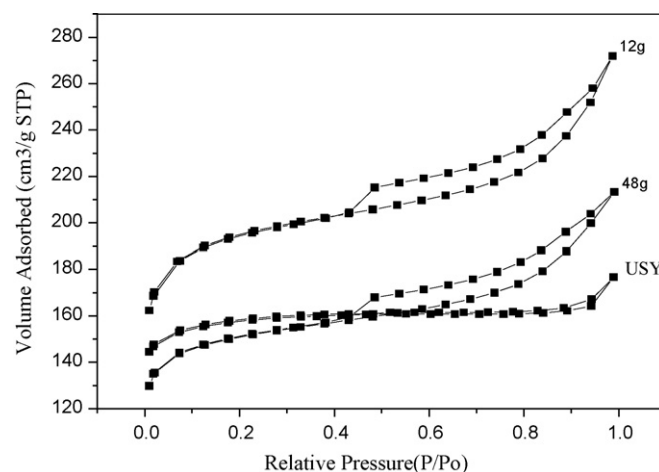
E	B		
	0.2	0.3	0.4
80	0.104	0.100	0.089
90	0.114	0.120	0.115
100	0.144	0.100	0.107

According to the  $F$  values, the rank of the significance was:  $D > E > B > C > B \times A > C > B \times E$ . Considering the interaction between  $B$  and  $C$ ,  $C1$  should be chosen, but the results of  $B1C1$  and  $B1C3$  were more or less the same. But from the single factor, result of  $C3$  was much bigger than that of  $C1$ , so  $C3$  was selected. Finally the optimal condition for combined modification of USY zeolites was  $A3B1C3D3E3$ . That is to say MHCA 0.4 mol/L, AP 0.2 mol/L, liquid–liquid ratio 1.5, 8 h and 100 °C.

## 3.2. Sample characterization

### 3.2.1. Surface area and pore distribution of modified USY

“USY” represented original USY samples, “12g” was the samples obtained from 250 mL flask as the reactor, “48g” was the products of 4 times scale-up experiment reacting in 1L autoclave. The same cases were as follows.

**Fig. 1.** N<sub>2</sub> adsorption–desorption isotherms of modified USY.

**Table 7**

Surface area and pore distribution of modified USY.

Sample	BET surface area, m <sup>2</sup> /g	Specific area of secondary pore by BJH, m <sup>2</sup> /g	Total pore volume, cm <sup>3</sup> /g	Volume of secondary pore by BJH, cm <sup>3</sup> /g
USY	481.97	41.55	0.273	0.049
12g	604.68	138.67	0.421	0.184
48g	466.26	105.58	0.330	0.145

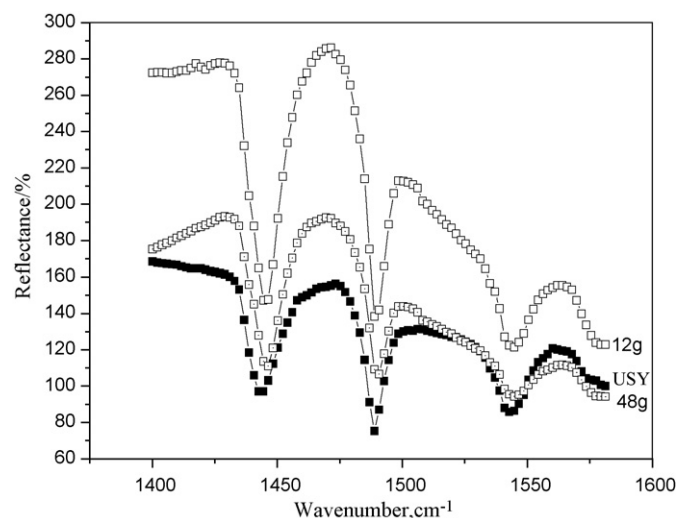
As can be seen from Fig. 1, N<sub>2</sub> adsorption–desorption isotherms of original USY was typical isotherm I. At the part of higher relative pressure, a loop occurred which indicated the existence of interstitial holes. It was clear that USY zeolites before modification had single channel structure that was composed basically of microporous pore. After modification, the modified USY had typical IV isotherms which indicated the appearance of mesopore structure. The volume of secondary pore was 0.184 cm<sup>3</sup>/g, 43.7% of the whole pore volume (in Table 7). However compared with the 12g-class samples, the surface area and pore volume of scale-up sample of 48g-class experiment decreased distinctly, this should be associated with the higher pressure, uneven stirring and excessive acidity in the 1 L autoclave. But its volume of secondary pore could still reach to 0.145 cm<sup>3</sup>/g—43.9% of the whole pore volume. Fig. 2 showed that modified USY zeolites had intensive distribution of secondary pores which focused on around 3.8 nm.

### 3.2.2. Fourier transform infrared (FT-IR) spectra of modified USY

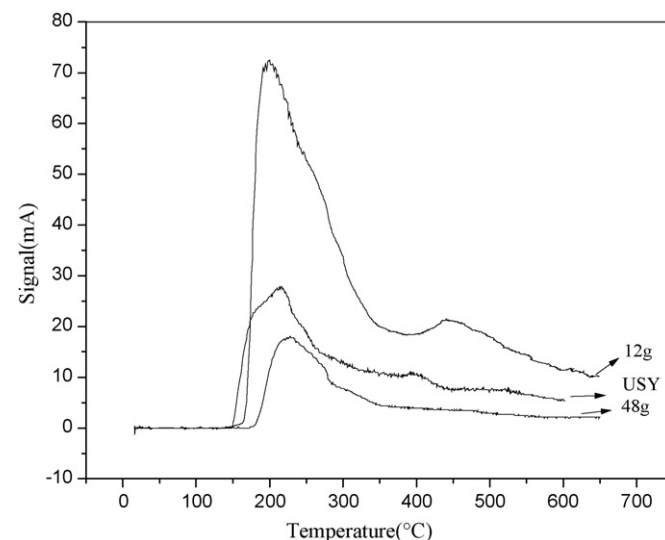
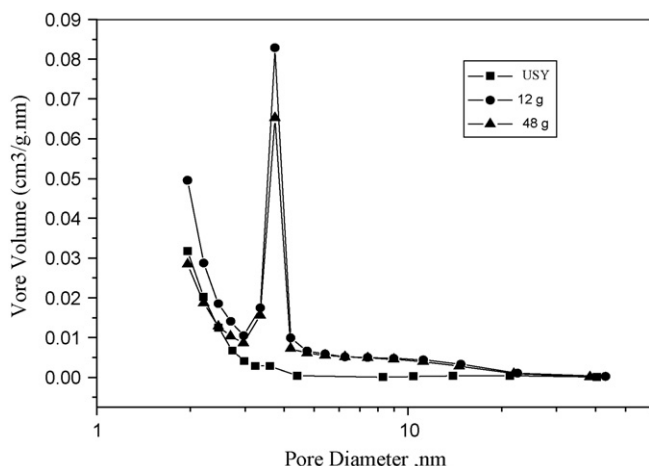
It was clear that there were three peaks on each curve in Fig. 3. 1442 and 1542 cm<sup>−1</sup> represented the characteristic peak of L and B acid, respectively while 1490 cm<sup>−1</sup> was the characteristic peak coming from the combined effect of B acid and L acid centers [46]. Compared with USY, the peak intensity of 12g-class modified samples increased significantly, indicating the increment of acid amounts both in B and L acid. For 48g-class scale-up test, the increment of L acid was less than that of 12g-class samples, and moreover a slight decrease in the peak intensity of B acid was observed, demonstrating the diminution of B acid sites.

### 3.2.3. Acid characterization of NH<sub>3</sub>-TPD

Compared with the original USY, 200 °C peak position of 12g-class modified USY shifted to low temperature while 400 °C peak position moved to high temperature (Fig. 4). It showed that the acid strength of weak acid reduced, but medium strong acid increased. According to the peak area, the acid amount of both strong acid and weak acid increased. 200 °C peak position of 48g-class scale-up

**Fig. 3.** FT-IR diffuse reflection spectra of pyridine adsorption of modified USY.

samples was a little high-temperature shifted, indicating that the acid strength of weak acid was enhanced, but weak acid amount reduced, which might be profitable to avoid secondary cracking. The acid amount of weak and strong acid of 48g-class was reduced, and this result contradicted that of 12g-class which might be brought about by the adverse effects amplification. Firstly, high temperature and pressure reaction conditions in autoclave led to the collapse of zeolite structure and reduction of acid amount; Secondly, some graphite impurities was introduced to modified samples from rotating shaft, which made the samples become black; At last, stirring in autoclave was inadequate and heating rate was slower than that of water bath.

**Fig. 4.** NH<sub>3</sub>-TPD profile of modified USY.**Fig. 2.** The pore size distribution of mesopore volume of modified USY by BJH.



**Table 8**

Crystal structural parameters of modified USY.

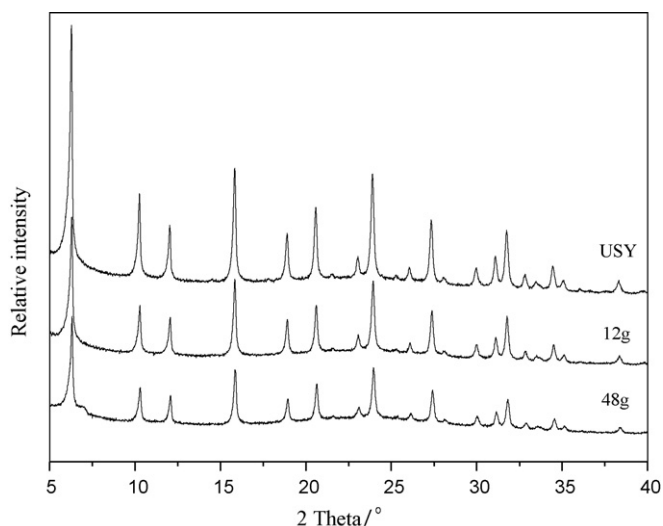
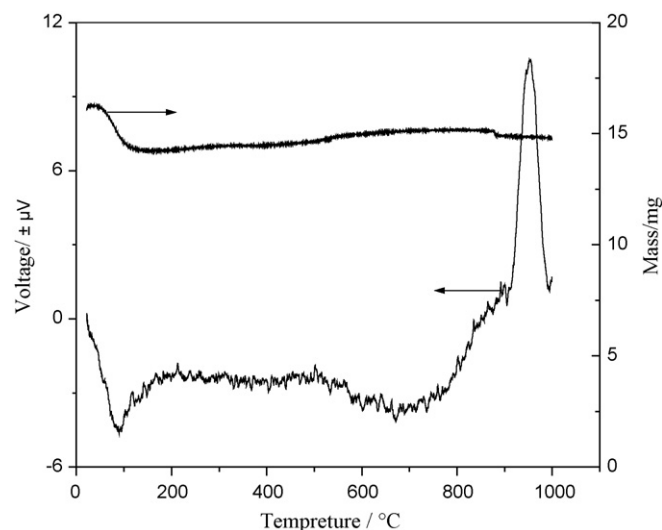
Sample	SiO <sub>2</sub> /Al <sub>2</sub> O <sub>3</sub>	Degree of crystallinity (C <sub>RX</sub> /%)	Cell parameters (a <sub>0</sub> /nm)
USY	8.9	50.3	24.4978
12g-class	17.0	36.7	24.3668
48g-class	19.0	27.1	24.3569

### 3.2.4. XRD-ray diffraction analysis

Table 8 gave us the crystal structure parameters of USY samples before and after modification. Compared with original USY, the Si–Al ratio of the modified samples increased significantly, unit cell parameters became smaller and crystallinity decreased. The improvement of Si–Al ratio was in certain extent due to dealumination and silicon reinsertion; Besides, insertion in framework of phosphoric acid hydrolysed by phosphate should also be taken into account. Because aluminum atoms could connected phosphorus atoms through oxygen bridge bonds [47], so the Si–Al ratio might include the contribution of P–Al ratio. Unit cell parameters became smaller which may be attributed to the replacement of aluminum by silicon or phosphorus, for both Si–O bond length and P–O bond length are shorter than Al–O bond length. Significant decrease in crystallinity was ascribed to the appearance of mesopore caused by the interpenetration of micropore and meanwhile some local collapse. In Fig. 5, we could see the modified samples still keep the characteristic peaks of USY, but the relative intensity was much weaker than parent USY. It should be noticed that the crystallinity of 48g-class modified USY was even lower than that of 12g-class modified samples. The reasons might be that the starting concentration and volume of acid in autoclave was stoichiometric composition as that in flask, but acid strength was different. Besides, the pressure in autoclave was higher than that in flask, so both might be the induction factors of the easier collapse of USY samples in scale-up test.

### 3.2.5. TG–DTA analysis of 48g-class scale-up test

As can be seen from the TG curve of 48g-class modified USY sample (Fig. 6), a peak of mass loss occurred around 100 °C indicating the removal of physically adsorbed water, and then its quality remained stable. A corresponding endothermic peak also appeared at 100 °C in the DTA curve, while the wide exothermic peak from 100 to 500 °C might come from the condensation of residual phosphorus hydroxyl on the zeolites surface and the collapse peak of

**Fig. 5.** X-ray diffraction patterns of modified USY zeolites.**Fig. 6.** TG–DTA curve of 48g-class scale-up test.**Table 9**

Hydrocracking performance of catalyst.

Product distribution, %	Modified catalyst	Commercial catalyst
HK-140 °C	16.07	18.68
140–370 °C	66.04	60.42
>370 °C	16.90	20.16
Loss	0.99	0.74
Conversion of >350 °C feedstock, %	75.7	75.0
Selectivity to middle distillate, %	80.43	76.38

Conversion =  $(1 - >350\text{ °C fraction of production} / >350\text{ °C fraction of feed oil}) \times 100\%$ .  
Yield =  $(140\text{--}370\text{ °C middle distillates fraction of production}) \times 100\%$ .  
Middle distillates selectivity =  $(140\text{--}370\text{ °C fraction of production} / <370\text{ °C fraction of production}) \times 100\%$ .

zeolite structure was not observed until 800 °C. This showed that the thermal stability of combined modified zeolite was enough to meet the requirement of industrial hydrocracking (<430 °C).

### 3.3. Evaluation of catalyst

As it can be seen from Table 9, under the 75.7% conversion of >350 °C feedstock, modified catalyst exhibited excellent hydrocracking performance. The 140–370 °C middle distillate yield of hydrocracking product was 66.04%, and at the same time, the selectivity to middle distillate could reach up to 80.43%. Compared with commercial catalyst, the yield and selectivity were increased by 5.62% and 4.05%, respectively. This result showed that combined modification of ultra-stable Y zeolites using multi-hydroxyl carboxylic acid and phosphate could meet the need of productive middle distillate in the industrial unit, which predicted it might be a potentially industrialized method of Y zeolites modification.

## 4. Conclusion

It is available to achieve combined dealuminum modification of USY zeolites using multi-hydroxyl carboxylic acid (MHCA) and phosphate (AP). According to L<sub>27</sub>(3<sup>13</sup>) orthogonal experiment, when the optimum modification condition was operated under 100 °C lasting 8 h with MHCA 0.4 mol/L, AP 0.2 mol/L and liquid–liquid ratio 1.5, the modified USY samples had developed secondary pore 0.184 mL/g, 43.7% of the whole pore volume and appropriate acid distribution as well as good crystallinity. For 1 L

scale-up test, the results showed that the pore volume of modified samples could reach 0.145 mL/g, 43.9% of the whole pore volume and an intensive distribution of secondary pores focusing on 3.8 nm around. The amount and intensity of medium strong acid as well as the thermal stability of modified USY were favorable. After performance evaluation, the 140–370 °C middle distillate yield was 66.04%, and middle distillate selectivity could reached up to 80.43%. Compared with commercial catalyst, the yield and selectivity were increased by 5.62% and 4.05%, respectively.

## References

- [1] G.-X. Yao, *Techno-Econ. Petrochem.* 16 (1) (2000) 10–15, 39.
- [2] S.-Z. Guo, F.-C. Wang, J.-L. Zhu, Y.-F. Liu, *Refining Chem. Ind.* 18 (4) (2007) 7–10.
- [3] *International Petroleum Economics* 5 (2009) 75–77.
- [4] G.T. Kerr, G.F. Shipman, *J. Phys. Chem.* 72 (8) (1968) 3071–3702.
- [5] X. Zhang, H.-Y. Zhu, J.-W. Zhang, *Petrol. Process. Petrochem.* 28 (5) (1997) 21–24.
- [6] G. Engelhardt, U. Lohse, V. Patzelová, M. Mägi, E. Lippmaa, *Zeolites* 3 (3) (1983) 233–238.
- [7] G. Engelhardt, U. Lohse, V. Patzelová, M. Mägi, E. Lippmaa, *Zeolites* 3 (3) (1983) 239–243.
- [8] H.-X. Wang, J.-Q. Fu, W.-M. Song, J.-r. Zhang, *Petrochem. Technol.* 26 (5) (1997) 302–305.
- [9] J.-G. Shao, S.-Y. Xiao, Z.-Y. Meng, *Chin. J. Catal.* 13 (1) (1992) 74–78.
- [10] M.J. Hey, A. Nock, R. Rudham, I.P. Appleyard, G.A.J. Haines, R.K. Harris, *J. Chem. Soc., Faraday Trans. 1* 82 (1986) 2817–2824.
- [11] P. Xie, Y.-Z. Zhang, L.-B. Zheng, *Chin. J. Catal.* 14 (4) (1993) 300–306.
- [12] A. Corma, V. Fornes, F. Rey, *Appl. Catal.* 59 (1) (1990) 267–274.
- [13] R. López-Fonseca, B. de Rivas, J.I. Gutiérrez-Ortiz, A. Aranzabal, J.R. González-Velasco, *Appl. Catal. B* 4 (2003) 31–42.
- [14] Z.-H. Wang, Y.-K. Lu, *Acta Petrolei Sinica (Petrol. Process. Sect.)* 14 (4) (1994) 9–17.
- [15] R.-G. Ding, Z.-F. Yan, L. Qian, X.-M. Liu, *Speciality Petrochem.* 3 (2) (1998) 24–27.
- [16] P. Xie, Y.-Z. Zhang, L.-B. Zheng, *Chin. J. Catal.* 14 (5) (1993) 407–410.
- [17] A.G. Panov, V. Gruver, J.J. Fripiat, *J. Catal.* 168 (1997) 321–327.
- [18] G.T. Kerr, *J. Phys. Chem.* 72 (7) (1968) 2594–2596.
- [19] D. Jerzy, K. Jacek, S. Bogdan, *Catal. Lett.* 25 (1994) 403–404.
- [20] N. Katada, Y. Kageyama, K. Takahara, T. Kanai, H.A. Begum, M. Niwa, *J. Mol. Catal. A: Chem.* 211 (2004) 119–130.
- [21] D. Jerzy, K. Waclaw, K. Jacek, S. Bogdan, *Catal. Lett.* 19 (1993) 159–165.
- [22] R. Bezman, *Catal. Today* 13 (1) (1992) 143–156.
- [23] R. Dimitrijevic, W. Lutz, A. Ritzmann, *J. Phys. Chem. Solids* 67 (2006) 1741–1748.
- [24] W. Lutz, H. Toufar, D. Heidemann, N. Salman, C.H. Rüschler, T.M. Gesing, J.-Chr. Buhl, R. Bertram, *Micropor. Mesopor. Mater.* 104 (2007) 171–178.
- [25] A. Yoshida, K. Inoue, Y. Adachi, *Zeolites* 11 (3) (1991) 223–231.
- [26] S.-T. Dong, X.-W. Li, D.-D. Li, Y.-H. Shi, H. Nie, X.-H. Kang, *Acta. Phys. Chim. Sin.* 18 (3) (2002) 201–206.
- [27] D.W. Breck, G.W. Skeels, in: G.C. Bond, P.B. Wells, F.C. Tompkins (Eds.), *Proc. 6th int. Congr. Catalysis*, vol. 2, Chemical Society, London, 1976, p. 645.
- [28] X.-M. Liu, L. Qian, Z.-F. Yan, *J. Petrochem. Univ.* 10 (4) (1997) 26–30.
- [29] A.P. Matharu, L.F. Gladden, S.W. Carr, *Stud. Surf. Sci. Catal.* 94 (1995) 147–154.
- [30] R. López-Fonseca, B. de Rivas, J.I. Gutiérrez-Ortiz, J.R. González-Velasco, *Stud. Surf. Sci. Catal.* 144 (2002) 717–722.
- [31] G. Pál-Borbély, H.K. Beyer, *Phys. Chem. Chem. Phys.* 5 (2003) 2145–2153.
- [32] G. Pál-Borbély, H.K. Beyer, *Phys. Chem. Chem. Phys.* 5 (2003) 5544–5551.
- [33] M.A. Zanjanchi, A. Ebrahimian, *Mater. Chem. Phys.* 110 (2008) 228–233.
- [34] S.K. Sur, R.G. Bryant, *Zeolites* 16 (1996) 118–124.
- [35] H. Pavol, J. Vladimír, S. Agáta, Ž. Zdenek, *React. Kinet. Catal. Lett.* 60 (1) (1997) 15–19.
- [36] Z.-M. Yan, D. Ma, J.-Q. Zhuang, X.-C. Liu, X.-M. Liu, X.-W. Han, X.-H. Bao, F.-X. Chang, L. Xu, Z.-M. Liu, *J. Mol. Catal. A: Chem.* 194 (2003) 153–167.
- [37] P. Panneerselvam, N. Thinakaran, K.V. Thiruvankataravi, M. Palanichamy, S. Sivasenan, *J. Hazard. Mater.* 159 (2008) 427–434.
- [38] A. Smieskov, J. Bocan, P. Hudec, Z. Zidek, *Zeolites* 14 (7) (1994) 553–556.
- [39] Th. Gross, U. Lohse, G. Engelhardt, K.-H. Richter, V. Patzelová, *Zeolites* 4 (1) (1984) 25–29.
- [40] A.C. Leiras Gomes, E. Falabella S-Aguiar, S. Cabral Menezes, D. Cardoso, *Appl. Catal. A: Gen.* 148 (1997) 373–385.
- [41] K.S. Triantafyllidis, S.A. Karakoulia, D. Gournis, A. Delimitis, L. Nalbandian, E. Maccallini, P. Rudolf, *Micropor. Mesopor. Mater.* 110 (2008) 128–140.
- [42] X. Zhang, X.-B. Ma, *Chem. Ind. Eng.* 24 (2) (2007) 145–149.
- [43] X.-J. Zhang, Z.-X. Wang, A.-U. Guo, Z.-S. Yuan, F.-C. Wang, *J. Fuel Chem. Technol.* 36 (5) (2008) 606–609.
- [44] X.-M. Liu, Z.-F. Yan, *Catal. Today* 68 (2001) 145–154.
- [45] B.-J. Liu, M. Li, Z. Feng, *Chin. J. Mol. Catal.* 21 (4) (2007) 300–303.
- [46] J.A. Lercher, G. Rimplmayr, *Appl. Catal.* 25 (1–2) (1986) 215–222.
- [47] Q. Chen, B.-x. Shen, H. Ling, *J. East China Univ. Sci. Technol. (Natural Science Edition)* 32 (4) (2006) 381–384.